OFFICE OF NAVAL RESEARCH

Contract N7onr-35801

T. O. I.

NR-041-032

LARGE PLASTIC DEFORMATIONS OF BEAMS UNDER BLAST LOADING

by

P. S. Symonds

GRADUATE DIVISION OF APPLIED MATHEMATICS

BROWN UNIVERSITY

PROVIDENCE, R. I.

December, 1953

Ali-99

A11-99

LARGE PLASTIC DEFORMATIONS OF BEAMS UNDER BLAST TYPE LOADING*

By

P. S. Symonds# (Brown University)

Abstract

Plastic deformations of supported beams under dynamic loading are determined under the assumption of negligible elastic strains. Particularly simple solutions are in several cases obtained when the load-time curve is of a class defined in the paper which includes typical blast pressure curves and rectangular pulses as simple examples.

1. Introduction

This paper treats some fundamental problems of structures subjected to strong dynamic loading, namely those of a simply supported or built-in uniform beam loaded by a uniform pressure or by a concentrated central force which is a specified function of time. The motion of an elastic beam under such conditions can be found without difficulty by standard beam vibration theory. However, if the load reaches high enough magnitudes to stress the beam beyond its elastic limit, a complete analysis becomes very much more difficult even when the post-elastic behavior is assumed to be of the simplest "ideally-plastic" type. In the present paper relatively simple solutions for the plastic deformations are obtained by making the further basic assumption that elastic deformations are negligible compared to plastic ones, and retaining the assumption of ideally plastic behavior.

---

* The results presented in this paper were obtained in the course of research sponsored by the Office of Naval Research under Contract N7onr-35801 with Brown University.

Associate Professor of Engineering.

This type of analysis is expected to be valid for ductile metals when the plastic deformations are much larger than the elastic ones. The beam is assumed to obey a "rigid-ideally-plastic" type of moment-curvature relation according to which no deformation occurs if the bending moment is less in magnitude than the limit moment M_o, corresponding to full plasticity over the cross-section; but while the moment has the value $\pm M_o$ indefinitely large changes of curvature can occur at constant moment. This corresponds to formation of a "plastic hinge" where discontinuities in slope angle can occur. The concept of plastic hinge action has been applied in various problems of dynamic loading of beams [1-6]* and of impact of beams [7,8]. A criterion was discussed in earlier papers [1,8] for the validity of the results, based on the hypothesis that the plastic-rigid method is suitable when the total energy absorbed sufficiently exceeds the maximum elastic strain energy that can be stored in the beam. Forms of this criterion appropriate in the present problems are given in this paper.

We discuss the following four problems in this paper (Fig. 1(a)):

Case I: Simply supported beam with uniformly distributed load;

Case II: Built-in beam with unformly distributed load;

Case III: Simply supported beam with concentrated load at mid-point;

Case IV: Built-in beam with concentrated load at mid-point.

---

* Numbers in brackets refer to the Bibliography.

In all cases the main principles of the solution are the same. However, the details differ considerably in different cases. Thus a numerical integration (either of a second order differential equation or of a system of first order equations) is generally required to solve case III, for which the analysis resembles those given in [2], [8]. However complete solutions for cases I, II and IV can be written in terms of simple definite integrals involving the load-time function; this is true regardless of the magnitude of the load provided the load-time function P(t) is one such that the total impulse up to any time t is at least as great as the product tP(t) of the instantaneous time and load values. Thus simple solutions are found for cases I, II, IV under the assumption

$$\int_0^t P\,dt \geq tP(t) \qquad (1)$$

The simplest examples of load functions which satisfy this relation are those in which P starts at its maximum value at t = 0 and then steadily decreases, (Fig. 1). Thus the simple analysis applies to loading curves which resemble typical blast pressure waves except that the actual rapid rise to a maximum is assumed to take place instantaneously. For convenience the class of P(t) functions satisfying the above inequality will be referred to in this paper simply as "blast type" loads.

Rectangular pulses are included in this category. The solutions for these involve the simplest arithmetic of all pulse forms, and are useful because it is found empirically that they

give good estimates (on the high side) of the deformations which would be produced by a pulse of any shape but with the same maximum load value and the same total impulse. Comparisons between results for rectangular, triangular and exponential pulses are given in the paper to exemplify this.

In all cases several different types of deformation may occur. For example, a simply-supported beam with distributed load might deform with a plastic hinge at the mid-point, the two halves rotating as rigid bars. This is the configuration in which quasi-static deformation would occur with the load at the statical collpase or "limit load" magnitude; hence it would be expected that for load intensities somewhat above the static collapse value the deformations would occur in this configuration. However, other types of configuration may occur in the course of a given load pulse. The configuration which a beam assumes at a given instant depends both on the instantaneous load magnitude and on the prior loading history.

The first step in attacking a problem is to assume a deformation configuration. This involves assuming positions of plastic hinges which divide up the beam into a number of segments. In each segment the bending moment is assumed either to be less than M_o in magnitude everywhere or to be equal to $\pm M_o$ at all points. In the former case the segment moves as a rigid bar, while in the latter case the segment is a finite plastic region in which particles move independently of one another, since there are no transverse shear forces. For any configuration the dynamical equations can be written for the various segments. These

will involve as unknowns the transverse and angular accelerations of the segments in which $|M| < M_o$ and also usually coordinates for the instantaneous positions of plastic hinges or interfaces between rigid-bar segments and finite plastic regions. The displacements must be continuous and this can be shown [1] to mean that transverse velocities also are continuous; transverse accelerations however are generally discontinuous at a moving plastic hinge or at a moving rigid-plastic interface.

The dynamical equations together with suitable (explicit or implicit) statements of continuity of transverse velocities can be solved for any chosen configuration. The solution is correct if and only if the bending moment furnished by the solution has actually a maximum magnitude less than M_o in the interior of every rigid-bar segment, as was assumed. If this is not the case another configuration must be chosen and analyzed in a similar manner.

Although a strict check on moment magnitudes cannot be made until the equations of motion are solved, it is highly desirable to sketch some representative moment diagrams for the rigid-bar segments at the start of the analysis of a configuration. The loading on each of these segments consists in part of known external loads and in part of linearly varying d'Alembert forces arising from the linear and angular accelerations of the segment. Hence the shear and bending moment diagrams can be drawn for various possible conditions and much information concerning the range of validity of a given configuration can be

quickly obtained. This will be exemplified in the analyses which follow.

It is sometimes advantageous to write the equations of impulse = momentum and angular impulse = moment of momentum for the whole or half beam, comprising several segments. These equations involve velocities rather than accelerations and hence the continuity conditions can be implicitly expressed in them. In general the dynamical equations of rigid body motion of individual segments are also needed, relating instantaneous external forces and moments on a segment to linear and angular accelerations of the segment. Either impulse - momentum equations or explicit velocity continuity equations may be combined with the dynamical equations of the rigid bar segments (whenever moving plastic hinges or elastic-rigid interfaces are concerned). Sometimes the impulse-momentum equations furnish directly the complete solution in very simple form, as in Case IV of this paper.

The solution for Case I is given in sufficient detail to indicate the analysis which would be required under the most general loading conditions and to make clear why the assumption of blast type loading (as defined above) considerably simplifies the analysis. The treatments of the other three cases are given much more briefly with consideration restricted, for loads of high magnitude, to blast type loading.

2. Case I: Simply Supported Beam, Uniform Load.

Consider a simply supported beam of constant limit moment M_o and mass per unit length m which is subjected to a load P(t)

uniformly distributed over the beam. On the assumption of "plastic-rigid" behavior of the beam no deflection occurs until the load P reaches a value large enough to bring the maximum statical moment up to the limit moment magnitude M_o. Thus no deflection occurs until $(M)_{max} = P\ell/4 = M_o$. It is convenient to introduct a dimensionless load parameter μ defined by $\mu = P\ell/M_o$. The critical value μ_I above which deflections begin is thus given by

$$\mu_I = 4. \tag{2}$$

For μ somewhat exceeding 4, deformation proceeds with a plastic hinge at the mid-point, each half of the beam rotating as a rigid body. (Fig. 2(b)). Writing the angular velocity and acceleration of the left-hand half as ω , $\dot{\omega}$ (positive clockwise) the equation of motion is

$$\frac{m\ell^3}{M_o}\ \dot{\omega} = \frac{3}{4}(\mu - 4). \tag{3}$$

Motion of this type will continue only so long as the maximum moment in each half is less in magnitude than M_o. The second critical load value, above which the configuration of Fig. 2(b) is incorrect, can be derived best by consideration of the diagrams for distributed load q, shear V and moment M, defined as in Fig. 6(a). The distributed load consists of the uniform applied load of intensity $P/2\ell$ together with a linearly varying load proportional to the acceleration at each point, as indicated in Fig. 6(b) for the left-hand half beam.

If $m\ell\,\dot{\omega} < P/2\ell$ the diagrams of q, V and M are as indicated by the full curves in Fig. 6(c) - 6(e). However if $m\ell\,\dot{\omega} > P/2\ell$

the corresponding diagrams are as shown by the dashed curves in Figs. 6(c) - 6(e). In this case a violation of the plasticity condition must occur. The load value μ_{II} below which the configuration of Fig. 2(b) applies is thus found by setting

$$\frac{P}{2\ell} = m\ell\,\dot{\omega} = \frac{\ell^2}{M_o}\left(\frac{3}{4}\mu - 3\right) \tag{4}$$

and is found to be

$$\mu_{II} = 12. \tag{5}$$

For loads in the range $4 \leq \mu \leq 12$ the final deformations are easily obtained by integrating Eq. (3). The angular velocity is

$$\frac{m\ell^3}{M_o}\,\omega = \frac{3}{4}\,I - 3t \tag{6}$$

where

$$I(t) = \int_0^t \mu\,dt. \tag{7}$$

Deformation continues until the relative angular velocity at the plastic hinge is reduced to zero. This occurs at a time t_f such that

$$t_f = \frac{1}{4}\,I_f \equiv \frac{1}{4}\int_0^{t_f} \mu(t)\,dt. \tag{8}$$

The final angle θ_{of} of the middle line of the beam and final central deflection δ_f are given by

$$\frac{m\ell^3}{M_o}\,\theta_{of} = \frac{m\ell^2}{M_o}\,\delta_f = \frac{3}{4}\int_0^{t_f} I\,dt - \frac{3}{32}\,I_f^2. \tag{9}$$

For loads such that $\mu > 12$, the plastic hinge spreads so that there is a central finite plastic zone between two segments of length $\xi\ell$ which rotate as rigid bars and simultaneously decrease

in length as the load increases, Fig. 2(c). The rate of spreading of the plastic zone is just sufficient to prevent a violation of the plastic condition, and hence is governed by

$$q(\xi\ell) = m\xi\ell\dot{\omega} - \frac{P}{2\ell} = 0 \tag{10}$$

where the angular acceleration $\dot{\omega}$ is now determined by the equation of motion of the rotating rigid segment of length $\xi\ell$. This is

$$\frac{1}{3} m\ell^3\xi^3\dot{\omega} = \frac{P}{2\ell}\frac{\ell^2\xi^2}{2} - M_o. \tag{11}$$

Combining Eqs. (10) and (11) we obtain

$$\mu\xi^2 - 12 = 0 \tag{12}$$

$$4\sqrt{3}\,\frac{m\ell^3}{M_o}\,\dot{\omega} = \mu^{3/2}. \tag{13}$$

The above result holds only while the load is being steadily increased from zero. In addition to the requirements of equilibrium and of the limit moment condition it is also necessary to satisfy the requirements of geometrical compatibility; the displacement and velocity must be continuous functions. At a cross-section where a localized plastic hinge exists or where a finite plastic zone joins a segment accelerating as a rigid body it can be shown [1] that the transverse accelerations are generally discontinuous, the amount of the jump being related to the speed of the moving hinge or interface and the angular velocities, as follows:

$$\ddot{y}(x_h^-) - \ddot{y}(x_h^+) = -\dot{x}_h[\dot{\theta}(x_h^-) - \dot{\theta}(x_h^+)] \tag{14}$$

where x_h is the coordinate of the hinge or plastic-rigid interface and $\dot{x}_h$ is the time derivative of x_h; $\dot{\theta}(x_h^-) - \dot{\theta}(x_h^+)$ is the

difference between angular velocities of segments just to the left and just to the right, respectively, of the hinge or interface; and $\ddot{y}(x_h^-) - \ddot{y}(x_h^+)$ is the corresponding difference in acceleration. The quantities x, y, θ are chosen so that $\theta = \partial y/\partial x$.

In the present case continuity of velocities at the moving interface $x_h = \xi^\ell$ is easily shown to be preserved while the load is steadily increasing so that the interface moves only in one direction. In fact, according to the above analysis the difference in both accelerations and angular velocities across the interface is zero with ξ and $\dot{\omega}$ given by Eqs. (12) and (13); clearly the jump condition (14) is satisfied in these conditions. However, suppose the load reaches a maximum and decreases. If Eqs. (12) and (13) are used to compute ξ and $\dot{\omega}$ it will be found that while the jump in accelerations is zero that in angular velocities in general does not vanish, so that the jump condition (14) is violated. In this case Eq. (12) must be replaced by the following inequality:

$$\mu\xi^2 - 12 \leq 0 \qquad (15)$$

To complete the analysis we must use an alternative equation which expresses continuity of velocity at the moving plastic-rigid junction.

The most convenient method in this problem seems to be to combine the velocity continuity condition and the dynamical requirements by writing the equation of moment of momentum of the half-beam with respect to an axis at the support point, x = 0. This equation is

$$\int_{t_I}^{t} \frac{P\ell}{4}\,dt - M_o(t - t_I) = \int_0^{\ell} m\ddot{y}x\,dx \qquad (16)$$

where t_I is the time corresponding to the load μ_I at which the deformation begins; for later times the moment at the mid-point is constant at M_o until the deformation ceases. In evaluating the right-hand side of Eq. (16) we have $\dot{y} = \omega x$ for $x \leq \xi\ell$. Hence Eq. (16) can be written

$$\frac{1}{4}\int_{t_I}^{t} \mu dt - (t - t_I) = \frac{m\ell^3}{M_o}\,\frac{\omega\xi^3}{3} + \frac{m}{M_o}\int_{\xi\ell}^{\ell} \ddot{y}x\,dx. \qquad (17)$$

For arbitrary shapes of force pulse the last term in Eq. (17) must be evaluated by considering the history of each particle which at any given time is in the plastic zone. This can be done since Eqs. (12) and (13) apply while the load is increasing, and the acceleration of any particle while it is in the plastic zone is equal to $P/(2\ell m)$. Thus the velocity of each particle in the region $\xi\ell < x < \ell$ can be derived and Eqs. (17) and (11) can be integrated; in general a step-by-step numerical procedure will be needed.

It can now be seen that the numerical analysis is greatly simplified if the load-time function is such that the interface between rigid and plastic regions always moves in one direction, with $\dot{\xi} \geq 0$. Then we can write

$$\xi\ell < x \leq \ell: \quad \ddot{y} = \frac{P}{2\ell m}, \quad \dot{y} = \int_0^{t} \frac{P}{2\ell m}\,dt \qquad (18)$$

We also have $t_I = 0$, and find that Eq. (17) reduces to

$$\frac{1}{4}\,\xi^2 \int_0^{t} \mu dt - t = \left(\frac{m\ell^3}{M_o}\right)\frac{1}{3}\,\omega\xi^3. \qquad (19)$$

After differentiation of Eq. (19) and combination with Eq. (11) we obtain results (in terms of $I(t) \equiv \int_0^t \mu dt$) as follows:

$$\xi^2 = \frac{12t}{I} \tag{20}$$

$$(\frac{m\ell^3}{M_o})^2 \omega^2 = \frac{I^3}{48t} \tag{21}$$

How we must investigate the conditions of loading such that $\dot{\xi} \geq 0$, and verify that the plasticity condition (15) remains satisfied. First we find by differentiating Eq. (20) that

$$2\xi \dot{\xi} = \frac{12}{I}(1 - \frac{t\mu}{I}). \tag{22}$$

This shows that $\dot{\xi} \geq 0$ if the load is of the "blast type" defined above by Eq. (1). Combining (22) with (20) we obtain

$$\mu\xi^2 - 12 = -\frac{24t\dot{\xi}}{\xi}. \tag{23}$$

Hence in view of Eq. (22) the necessary inequality (15) is always satisfied when the loading is of this general type.

The initial position of the rigid-plastic interface can be obtained from Eq. (20) by examining the limit of the quotient at $t = 0$, and $\xi(0) \equiv \xi_o$ is found to be given by

$$\xi_o^2 \mu_o = 12 \tag{24}$$

as would be expected from the discussion leading to Eq. (12).

The formulas (20) and (21) apply, of course, only while the plastic region exists, i.e., until the time t_s when $\xi = 1$, where

$$t_s = \frac{I_s}{12} \equiv \frac{1}{12}\int_0^{t_s} \mu \, dt. \tag{25}$$

The corresponding angular velocity ω_s is given by

$$\frac{m\ell^3}{M_o}\,\omega_s = \frac{1}{2}\,I_s. \tag{26}$$

The mid-point displacement δ_s at this instant is readily found by integrating the known acceleration $P/2\ell m$ to be

$$\frac{m\ell^2}{M_o}\,\delta_s = \frac{1}{2}\int_0^{t_s} I\,dt. \tag{27}$$

In the final stage of the motion there is a hinge at the mid-point only, as in Fig. 2(b). The angular velocity of the half-beam is given by Eq. (19) after setting $\xi = 1$, i.e. by Eq. (6). The plastic deformation is completed at the time t_f such that $\omega(t_f) = 0$; thus

$$t_f = \frac{1}{4}\,I_f \tag{28}$$

and we can express the final displacement δ_f of the mid-point as

$$\frac{m\ell^2}{M_o}\,\delta_f = \frac{1}{2}\int_0^{t_s} I\,dt + \frac{3}{4}\int_{t_s}^{t_f} I\,dt - \frac{3}{32}\left[I_f^2 - \frac{1}{9}\,I_s^2\right] \tag{29}$$

The final shape of the beam is indicated in Fig. 2(d). A discontinuity in the slope angle appears at the mid-point (and under rectangular load pulses also at $\xi_o\ell$). The final central angle θ_{of} is obtained by integrating Eq. (5) in the time interval t_s to t_f:

$$\frac{m\ell^3}{M_o}\,\theta_{of} = \frac{3}{4}\int_{t_s}^{t_f} I(t)dt - \frac{3}{2}(t_f^2 - t_s^2). \tag{30}$$

The final angle θ_{1f} at the support is equal to θ_{of} plus the value attained in the time interval 0 to t_s, which is readily computed

by means of Eq. (21). We have

$$\frac{m\ell^3}{M_o}\,\theta_{1f} = \frac{1}{4\sqrt{3}}\int_0^{t_s}\left(\frac{I^3}{t}\right)^{1/2} dt + \frac{m\ell^3}{M_o}\,\theta_{of}. \tag{31}$$

The change of curvature of an element of length dx at any point in the zone where plastic yielding has taken place occurs only in the small increment of time dt during which the interface between rigid and plastic material is traversing it. Hence if the interface is at $\xi\ell$ at a given instant the permanent curvature acquired by an element of length $dx = \dot{\xi}\, d\ell$ at this position is

$$\frac{1}{\ell}\frac{d\theta}{d\xi} = \omega\frac{dt}{dx} = \frac{\omega}{\dot{\xi}\ell}. \tag{32}$$

By use of Eqs. (20) - (22) we can express the curvature as

$$\frac{m\ell^3}{M_o}\frac{d\theta}{d\xi} = \frac{I^2}{12 - \mu\xi^2} = f(\xi). \tag{33}$$

Here the right-hand side is to be regarded as a function of ξ rather than of time, since the ξ - t relation is given implicitly by Eq. (20). An integration with respect to ξ between limits ξ_o and 1 yields the angle difference $\theta_{1f} - \theta_{of}$, and can be used as a check. A second integration would lead to deflection values in the region of permanent deformations.

It should be emphasized that both Eqs. (32) and (33) hold only under loading conditions such that $\dot{\xi} > 0$. If μ is constant (non-zero) ξ has the constant value ξ_o furnished by Eq. (24), and the curvature is infinite, as is usual at a stationary plastic hinge or rigid-plastic interface.

To illustrate typical results we now give formulas for deformations for the case of a rectangular load pulse with amplitude μ_o and duration time τ. Results for this and for two other shapes of load curve are shown graphically in Figs. 7-9, where dimensionless deformations are plotted in a way which makes the results quite insensitive to the shape of the load-time curve, as discussed later.

For the rectangular load pulse we have

$$0 \leq t \leq \tau \qquad I(t) = \mu_o t \tag{34a}$$

$$t > \tau \qquad I(t) = \mu_o = \text{constant}. \tag{34b}$$

Hence Eqs. (25) and (28) yield

$$t_s = \frac{1}{12}\mu_o\tau; \quad t_f = \frac{1}{4}\mu_o\tau. \tag{35}$$

For low loads ($\mu_o < 4$) no appreciable permanent deformation takes place. For medium loads ($4 \leq \mu \leq 12$) we use Eqs. (7) - (9) and obtain

$$\frac{m\ell^3}{M_o}\theta_f = \frac{m\ell^2}{M_o}\delta_f = \frac{3}{32}\mu_o(\mu_o - 4)\tau^2. \tag{36}$$

For high loads ($\mu_o \geq 12$) we use Eqs. (29) - (33) and find

$$\frac{m\ell^3}{M_o\tau^2}\theta_{of} = \frac{\mu_o^2}{24} \tag{37a}$$

$$\frac{m\ell^3}{M_o\tau^2}\theta_{1f} = \frac{\mu_o}{8}(\mu_o - \sqrt{3\mu_o}) \tag{37b}$$

$$\frac{m\ell^2}{M_o\tau^2}\delta_f = \frac{\mu_o}{12}(\mu_o - 3). \tag{37c}$$

The final curvature is found by inserting $\mu = 0$, $I = \mu_o\tau$ in Eq. (33), and thus the change in angle $\Delta\theta$ across the segment

from $\xi_o \ell$ to ℓ is given by

$$\frac{m\ell^3}{M_o} \Delta\theta = \int_{\xi_o}^{1} \frac{d\theta}{d\xi} \, d\xi = \frac{\mu_o^2 \tau^2}{12} (1 - \xi_o). \qquad (37d)$$

This angle change $\Delta\theta$ plus the angle of rotation $\theta_{1\tau}$ which occurs at the rigid-plastic interface during the time τ while the load is applied should equal the angle difference $\theta_{1f} - \theta_{of}$ as given by Eqs. (37). Taking $\xi_o^2 = 12/\mu_o$ we have

$$\frac{\mu_o^2 \tau^2}{12} \left(1 - \sqrt{\frac{12}{\mu_o}}\right) + \frac{1}{4\sqrt{3}} \int_0^{\tau} \mu_o^{3/2} \, t \, dt = \frac{\mu_o^2 \tau^2}{12} - \frac{\sqrt{3}}{8} \mu_o^{3/2} \tau^2.$$

This checks with the result obtained by subtracting Eq. (37a) from Eq. (37b).

A rather curious result is that the final angle θ_{of} of the tangent line at the mid-point is not a continuous function of the load amplitude μ_o at the value $\mu_o = 12$. By Eq. (36) we have

$$(\mu_o = 12 - 0): \qquad \frac{m\ell^3}{\mu_o \tau^2} \theta_{of} = \frac{3}{32} \times 12 \times 8 - 9.$$

Using Eq. (37a), however, we find

$$(\mu_o = 12 + 0): \qquad \frac{m\ell^3}{\mu_o \tau^2} \theta_{of} = \frac{12^2}{24} = 6.$$

It is readily verified that the angle θ_{1f} and the central deflection δ_f are continuous at $\mu_o = 12$. The explanation for the abrupt decrease in θ_{of} at this value lies in the fact that for any load such that μ_o exceeds 12, however slightly, there is a segment of length $2(1 - \xi_o)\ell$ at the middle of the beam which remains straight and undeformed during the time interval 0 to t_s. For $\mu_o < 12$, on

the other hand, the angle of the tangent at the mid-point increases steadily during the whole of the time interval 0 to t_f. The discontinuity affects only a line segment of infinitesimal length, and the overall deformation is, in fact, a continuous function of μ_o, as shown by the smooth rise of θ_{1f} and δ_f.

The energy absorbed in plastic deformations is of interest. For medium loads ($\mu_o < 12$) this is the work done by the limit moment at the central plastic hinge and hence is

$$\mu_o \leq 12: \qquad E_p = 2M_o\theta_f = \frac{2M_o^2}{m\ell^3}\left[\frac{3\mu_o^2}{32} - \frac{3\mu_o}{8}\right]\tau^2. \tag{38a}$$

For high loads ($\mu_o > 12$) energy is absorbed at the central hinge, in the regions of continuous plastic deformation from $\xi_o\ell$ to ℓ, and at the stationary plastic-rigid interfaces at $\xi_o\ell$. Thus we have in this case

$$E_p = 2M_o[\theta_{of} + \Delta\theta + \theta_\tau] = 2M_o\theta_{1f}.$$

Hence

$$\mu_o \geq 12: \qquad E_p = \frac{2M_o^2}{m\ell^3}\left[\frac{\mu_o^2}{8} - \frac{\sqrt{3}}{8}\mu_o^{3/2}\right]\tau^2. \tag{38b}$$

The work done in plastic deformation E_p according to Eqs. (38) is a continuous function of μ_o, as expected.

In Figs. 7-9 curves are drawn for the central deflection δ_f, the central angle θ_{of} and the outer angle θ_{1f} for the three load types indicated in the figures, i.e., rectangular, triangular, and exponential. In all cases the dimensionless deflections $\frac{m\ell^2}{M_oT_o^2}\delta_f$, $\frac{m\ell^3}{M_oT_o^2}\theta_{of}$, and $\frac{m\ell^3}{M_oT_o^2}\theta_{1f}$ are plotted. Here T_o is defined as the time such that the product of T_o and the peak load

μ_o is equal to the total impulse, i.e., so that

$$\mu_o T_o = \int_0^\infty \mu dt \tag{39}$$

where μ_o is the peak load value in each case. Thus $T_o = \tau$ for the rectangular pulse of duration τ, while for the triangular pulse of duration τ the impulse is $\frac{1}{2}\mu_o\tau$ and $T_o = \frac{1}{2}\tau$. For an exponential pulse defined by $\mu = \mu_o e^{-t/\tau}$, the total impulse is $\tau\mu_o$ so that T_o is equal to τ, the time for the load to decrease from μ_o to μ_o/e.

The curves for these dimensionless variables plotted as functions of maximum load are found to lie quite close together, indicating that the total impulse $\mu_o T_o$ and maximum load μ_o mainly determine the final deformations, the precise shape of the load-time relation being relatively unimportant. Thus for a simply supported beam one can take the results for the rectangular pulse form as good estimates of the corresponding results for a force pulse of arbitrary shape, provided the peak load $\mu_o = P_{max}\ell/M_o$ is used in the formulas and τ is replaced by the time T_o such that $\mu_o T_o$ is the total impulse $\int_0^\infty \mu dt$. This will furnish an estimate which will generally be too high. The comparison of various force pulses acting on a free-free beam (reference [2]) led to the same conclusions as those stated above.

Signicant quantities expressing deformations due to rectangular load pulses are plotted in Figs. 10-13 for the four cases of loading and support considered in this paper.

3. Case II: Built-in Beam with Uniform Pressure Loading

The above analysis can be extended with only minor modifications to a beam with both ends fixed under uniformly distributed load, Fig. 3(a)). Deformations begin in this case when the end moments as well as the moment at the mid-point reach the magnitude M_o; hence the first critical load is

$$\mu_I = 8. \tag{43}$$

For medium loads plastic hinges are present at both ends and mid-point, and the angular acceleration $\dot{\omega}$ of the half-beam is given by

$$\frac{m\ell^3}{M_o}\dot{\omega} = \frac{3}{4}(\mu - 8). \tag{44}$$

An argument analogous to that of Section 2 leads to the result that a widening of the central hinge into a finite plastic zone must begin when the load reaches the second critical value μ_{II} where

$$\mu_{II} = 24. \tag{45}$$

Thus the deflections for loads in the range $8 \leq \mu \leq 24$ can be written as

$$\frac{m\ell^3}{M_o}\theta_f = \frac{m\ell^2}{M_o}\delta_f = \frac{3}{4}\int_0^{t_f} I\,dt - 3t_f^2 \tag{46}$$

where

$$t_f = \frac{1}{8} I_f \equiv \frac{1}{8}\int_0^{t_f} \mu dt. \tag{47}$$

The analysis for loads with $\mu > 24$ is based on the following momentum and acceleration equations, respectively

$$\int_{t_I}^{t} \frac{p\ell}{4} dt - 2M_o(t - t_I) = \int_0^{\ell} m\dot{y}x \, dx \tag{48}$$

$$\frac{m\ell^3}{M_o} \dot{\omega}\xi^3 = \frac{3}{4}\mu\xi^2 - 6. \tag{49}$$

The above replace Eqs. (16) and (11), respectively. In Eq. (48) t_I is the time at which μ reaches the value $\mu_I = 8$. If we again consider "blast type" loading (satisfying Eq. (1)) we arrive at the following results corresponding to those of Section 2:

$$\frac{m\ell^3}{M_o} \omega\xi^3 = \frac{3}{4} \xi^2 I - 6t \tag{50}$$

$$\xi^2 = \frac{24t}{I}; \quad \xi_o^2 = \frac{24}{\mu_o} \tag{51}$$

$$\left(\frac{m\ell^3}{M_o} \omega\right)^2 = \frac{I^3}{96t} \tag{52}$$

$$t_s = \frac{1}{24} I_s. \tag{53}$$

In the last phase of the motion, with hinges again only at mid-point and ends, we have

$$\frac{m\ell^3}{M_o} \omega = \frac{3}{4} I - 6t. \tag{54}$$

Thus the deformation is completed at the time t_f where

$$t_f = \frac{1}{8} I_f. \tag{55}$$

The final deformations for loads in the range $\mu_o \geq 24$ are given by the following formulas:

$$\frac{m\ell^3}{M_o} \theta_{of} = \frac{3}{4} \int_{t_s}^{t_f} I \, dt - 3(t_f^2 - t_s^2) \tag{56a}$$

$$\frac{m\ell^3}{M_o}\theta_{1f} = \frac{1}{4\sqrt{6}}\int_0^{t_s}\left(\frac{I^3}{t}\right)^{1/2} dt + \frac{m\ell^3}{M_o}\theta_{of} \tag{56b}$$

$$\frac{m\ell^2}{M_o}\delta_f = \frac{1}{2}\int_0^{t_s} I\,dt + \frac{3}{4}\int_{t_s}^{t_f} I\,dt - \frac{3}{64}\left(I_f^2 - \frac{1}{9}I_s^2\right) \tag{56c}$$

$$\frac{m\ell^3}{M_o}\frac{d\theta}{d\xi} = \frac{I^2}{24 - \mu\xi^2}\,. \tag{56d}$$

For this case the energy absorbed in plastic deformation E_p is given by

$$E_p = 4M_o\theta_{1f} \tag{57}$$

Deformations and E_p for rectangular force pulses are plotted in Figs. 10-13 in non-dimensional form.

4. Case III: Simply-Supported Beam with Concentrated Load

In this and the following section we outline the solutions for the plastic deformations of a simply supported beam and of a fixed-ended beam, respectively, loaded by a concentrated force P at the mid-point. These analyses turn out to be surprisingly different from each other, as well as from that found appropriate for cases I and II.

For the simply supported beam (Fig. 4(a)) the deformation begins when the load parameter $\mu = P\ell/M_o$ reaches the first critical value μ_I, where

$$\frac{P_I\ell}{M_o} = \mu_I = 2 \tag{58}$$

For μ not too greatly exceeding 2 deformation proceeds as in Fig. 4(b) with a plastic hinge at the mid-point. This configuration must be replaced by that of Fig. 4(c) when μ exceeds the

second critical value μ_{II} where

$$\mu_{II} = 18. \tag{59}$$

This second critical value is found by setting the minimum moment in the half-beam equal to $-M_o$ and solving the resulting cubic equation in μ. For loads with $\mu > 13$ plastic hinges occur at cross-sections $\xi\ell$ from the mid-point and the motion of these hinges must be investigated. With still larger loads in certain circumstances the configuration of Fig. 4(c) must be replaced by another in which the lateral hinges are spread into finite plastic regions. However it can be shown that with the blast type of loading defined by Eq. 1 this type of deformation does not occur.

Loads in the medium range $2 \leq \mu \leq 18$ produce an angular velocity ω of the left half-beam (Fig. 4(b)) given by

$$\frac{m\ell^3}{M_o}\,\omega = \frac{3}{2}\int_{t_I}^{t} \mu\, dt - 3(t - t_I) \tag{60}$$

where t_I is the time when the central hinge appears, corresponding to μ_I. Thus for loads of arbitrary pulse form with maximum between 2 and 18 the final deformations are

$$\frac{m\ell^3}{M_o}\,\theta_{cf} = \frac{mL^2}{M_o}\,\delta_f = \frac{3}{2}\int_{t_I}^{t_f} I_1(t)dt - \frac{3}{2}(t_f - t_I)^2 \tag{61}$$

where

$$I_1(t) = \int_{t_I}^{t} \mu\, dt \tag{62a}$$

and

$$t_f = \frac{1}{2}\, I_f \tag{62b}$$

The deformations caused by higher loads ($\mu_o > 18$) are governed by the dynamical equations of the two segments of length $\xi\ell$ and $(1-\xi)\ell$, respectively, together with the continuity condition at the hinge section. The angular accelerations $\dot{\omega}_o$, $\dot{\omega}_1$, obey the following equations:

$$\frac{m\ell^3}{M_o}\dot{\omega}_o = \frac{3\mu}{\xi^2} - \frac{24}{\xi^3} \tag{63a}$$

$$\frac{m\ell^3}{M_o}\dot{\omega}_1 = \frac{3}{(1-\xi)^3} \tag{63b}$$

The general equation (14) for the discontinuities at a moving hinge in this case yields the equation

$$\frac{\mu}{\xi} - \frac{12}{\xi^2} + \frac{3}{(1-\xi)^2} = -\dot{\xi}(\omega_o - \omega_1)\frac{m\ell^3}{M_o} \tag{64}$$

The angular velocities ω_o and ω_1 are defined as positive clockwise in the left half beam. Differentiation of Eq. (64) and substitution of the formulas for the angular accelerations $\dot{\omega}_o$, $\dot{\omega}_1$, leads to the following equation for the hinge coordinate ξ

$$\ddot{\xi}\left[\frac{\mu}{\xi} - \frac{12}{\xi^2} + \frac{3}{(1-\xi)^2}\right] - \dot{\xi}\left[\frac{3\dot{\xi}}{(1-\xi)^3} + \frac{2\mu\dot{\xi}}{\xi^2} + \frac{\dot{\mu}}{\xi}\right] = 0 \tag{65}$$

This equation can be integrated in analytic form if the load is a rectangular pulse. Then Eqs. (64) and (65) are satisfied during the pulse duration time τ with ξ = constant = ξ_o where

$$\frac{\mu_o}{\xi_o} - \frac{12}{\xi_o^2} + \frac{3}{(1-\xi_o)^2} = 0 \tag{66a}$$

For time $t > \tau$ with $\mu = \dot{\mu} = 0$ Eq. (65) reduces to

$$\ddot{\xi}\left[\frac{1}{(1-\xi)^2} - \frac{4}{\xi^2}\right] - \frac{\dot{\xi}^2}{(1-\xi)^3} = 0 \qquad (66b)$$

The solution of this equation can be found by standard methods. A first integration yields the result

$$\frac{1}{C}\frac{d\xi}{dt} = \frac{(2-\xi)(2-3\xi)^{1/3}}{1-\xi} \qquad (67)$$

where C is a constant. Integrating again we obtain

$$(t-\tau)C = \left[-\frac{\zeta^2}{2} + \frac{1}{2n}\log\frac{n^2-n\zeta+\zeta^2}{(n+\zeta)^2} + \frac{\sqrt{3}}{n}\tan\frac{-1+2\zeta}{n\sqrt{3}}\right]_{\zeta=(2-3\xi_o)^{1/3}}^{\zeta=(2-3\xi)^{1/3}} \qquad (68)$$

where $n = 4^{1/3}$, and ξ_o is the constant defined by Eq. (66a). The constant C is to be determined from the following equation:

$$C = \frac{3(2-3\xi_o)^{2/3}}{\frac{m\ell^3}{M_o}[\omega_o(\tau) - \omega_1(\tau)]\xi_o^2(1-\xi_o)} \qquad (69)$$

where $\omega_o(\tau)$ and $\omega_1(\tau)$ are the angular velocities at $t = \tau$ and are obtained in an obvious manner from Eqs. (63), the accelerations being constant for $t \leq \tau$.

For other than rectangular force pulses Eq. (65) is not easily integrable. It is found (as in the similar analysis described in [2]) that a more convenient basis for numerical integration is afforded by the equation of moment of momentum of the half-beam with respect to an axis at the support. This equation here takes the form

$$3\int_{t_I}^{t} \mu\, dt - 6(t - t_I) = \frac{m\ell^3}{M_o}\left[(\omega_o-\omega_1)(3\xi^2-\xi^3) + 2\omega_1\right] \qquad (70)$$

where t_I is the time at which the central hinge first appears, corresponding to $\mu_I = 2$. Thus $t_I = C$ for force pulses of the blast loading types we are considering. The step-by-step numerical solution of Eq. (70) is carried out in the manner described in detail in [2]. The left-hand side is first evaluated at a sequence of times. Then by trial and error the value of ξ at each step is found such that when ω_o and ω_1 are computed by applying Simpson's rule (or an equivalent integration formula) to the accelerations furnished by Eqs. (63), Eq. (70) is satisfied to the required accuracy.

The circumstances in which a new configuration appears with a finite plastic region in the interior of each half-beam can be found by studying the bending moment diagram for the inner segment of length $\xi\ell$. It is necessary that $d^2M/dx^2 \geq 0$ at the travelling hinge section; otherwise a moment less (algebraically) than $-M_o$ would occur in the interior of the segment. Hence we must have $\mu\xi - 12 \leq 0$ if the configuration of Fig. (4c) is to be valid. An inspection of Eq. (64) shows that this inequality is always satisfied for a rectangular load pulse or for a steadily decreasing load, in which case $\dot{\xi} > 0$, $\omega_o > \omega_1$.

Curves showing the final deformations (mid-point deflection δ_f, central angle θ_{of} and angle θ_{1f} at the support) and the plastic work E_p are shown in Figs. 10-13 for rectangular force pulses. The plastic work E_p is given by

$$E_p = 2M_o[\theta_{of} + (\theta_{of} - \theta_{1f})] \qquad (71)$$

5. Case IV: Built-in Beam with Concentrated Load

A beam with ends initially fixed as in Fig. 5(a) undergoes no deformation (according to the plastic-rigid hypothesis) under concentrated central loading if the load is less than $P_I = M_o \ell/4$. Thus the first critical value of the load parameter $\mu = P\ell/M_o$ is

$$\mu_I = 4 \tag{72}$$

When μ slightly exceeds 4 the beam deforms as indicated in Fig. 5(b) with plastic hinges at mid-point and ends, the two halves rotating as rigid bodies. This simple configuration must be replaced by another when the load reaches a sufficiently high value. The need for a new configuration becomes evident when the moment diagrams of the left half-beam are sketched, as for Case I. These show that a violation of the plasticity condition would first occur near the end support and that the critical load value is that which corresponds to the vanishing of the reaction force at the support. The reaction force R in this phase is given by the formula

$$\frac{R\ell}{M_o} = 3 - \frac{\mu}{4} \tag{73}$$

and hence the second critical value μ_{II} has the value

$$\mu_{II} = 12 \tag{74}$$

For loads in the medium range such that $4 \leq \mu \leq 12$ the angular velocity ω of the half-beam is given by the formula

$$\frac{m\ell^3}{M_o}\omega = \frac{3}{2}\int_{t_I}^{t} \mu \, dt - 6(t - t_I) \tag{75}$$

and the final deformations may be computed from the general equations

$$\frac{m\ell^3}{M_o}\theta_f = \frac{m\ell^2}{M_o}\delta_f = \frac{3}{2}\int_{t_I}^{t_f} I_1(t)dt - 3(t_f-t_I)^2 \qquad (76)$$

where $I_1(t) = \int_{t_I}^{t} \mu\, dt$, t_I is the time at which the motion begins, and t_f is found by setting $t = t_f$, $\omega = 0$ in Eq. 75.

When the load exceeds a value corresponding to $\mu_{II} = 12$ a new configuration of the type shown in Fig. 5(c) appears, the half-beam again comprising two segments with different types of motion. The inner segment, of length $\xi\ell$, has moment varying from $-M_o$ to M_o while the outer segment has the constant moment $-M_o$ throughout its length. Hence the inner segment rotates as a rigid body with angular velocity ω, while each particle of the outer segment moves with constant velocity, since there are no shear forces or external loads. Thus the outer segment is a plastic region of finite length.

We now restrict consideration to loads of blast type as defined by Eq. 1. Assuming that the initial load value is such that $\mu > 12$, the configuration immediately becomes that sketched in Fig. 5(c). The dependence of ξ on time can easily be found by writing the equations of linear and angular momentum for the half-beam. These involve as unknown quantities only the angular velocity ω of the inner segment and ξ, which increases from its initial value determined by the initial load to unity; as long as a particle is in a perfectly plastic segment it remains at rest since it had no initial velocity and no forces act on it. The equations of linear impulse-momentum and angular impulse - moment of momentum (with respect to the support point) take the following forms, respectively:

$$\int_0^t \mu\, dt = \frac{m\ell^3}{M_o}\omega\xi^2 \tag{77}$$

$$3\int_0^t \mu\, dt - 12t = \frac{m\ell^3}{M_o}\omega\,\xi^2(3-\xi) \tag{78}$$

But these may at once be combined so as to eliminate ω, yielding the following simple formula for ξ :

$$\xi = \frac{12t}{I} \tag{79}$$

where $I = \int_0^t \mu dt$. The initial value ξ_o of ξ is thus given by

$$\xi_o = \frac{12}{\mu_o} \tag{80}$$

where μ_o is the initial value of the load. The angular velocity is obtained by putting the above expression for ξ in Eq. (77); we have

$$\frac{m\ell^3}{M_o}\,\omega = \frac{I^3}{144\ t^2} \tag{81}$$

The formulas (77) - (81) hold until the time $t = t_s$ when ξ becomes unity; from Eq. (79) t_s is given by

$$t_s = \frac{I_s}{12} \tag{82}$$

The slope angle θ_{os} at the mid-point acquired in this time interval can thus be computed from the formula

$$\frac{m\ell^3}{M_o}\,\theta_{os} = \frac{1}{144}\int_0^{t_s} \frac{I^3}{t^2}\, dt \tag{83}$$

The central deflection δ_s at the instant $t = t_s$ may be determined from

$$\frac{m\ell^2}{M_o}\,\delta_s = \frac{1}{12}\int_0^{t_s} \frac{I^2}{t}\, dt \tag{84}$$

The subsequent motion ($t > t_s$) takes place according to the configuration of Fig. 5(b) with angular velocity given by Eq. (78) after setting $\xi = 1$ (or from Eq. (75) with $t_I = 0$), as follows:

$$\frac{m\ell^3}{M_o}\omega = \frac{3}{2} I(t) - 6t \tag{85}$$

the deformation is completed when $\omega = 0$ at a time $t = t_f$ such that

$$t_f = \frac{1}{4} I_f \tag{86}$$

Hence we can compute the final angles θ_{of} at the mid-point and θ_{1f} at the support and the final central displacement δ_f from the following formulas, when $\mu_o > 12$

$$\frac{m^3}{M_o}\theta_{of} = \frac{1}{144}\int_0^{t_s}\frac{I^3}{t^2}\,dt + \frac{3}{2}\int_{t_s}^{t_f} I\,dt - 3(t_f^2 - t_s^2) \tag{87a}$$

$$\frac{m\ell^3}{M_o}\theta_{1f} = \frac{3}{2}\int_{t_s}^{t_f} I\,dt - 3(t_f^2 - t_s^2) \tag{87b}$$

$$\frac{m\ell^2}{M_o}\delta_f = \frac{1}{12}\int_0^{t_s}\frac{I^2}{t}\,dt + \frac{3}{2}\int_{t_s}^{t_f} I\,dt - 3(t_f^2 - t_s^2) \tag{87c}$$

Here t_s and t_f are furnished by Eqs. (82) and (86), respectively. Curves showing the final deformations and the plastic work as functions of μ_o are presented in Figs. 10-13 for rectangular pulses. These can be used to estimate results for other pulse shapes by substituting T_o for τ, T_o being defined by Eq. 39. The plastic work E_p is here given by

$$E_p = 2M_o\theta_{of} \tag{88}$$

6. Discussion of Results

Newmark [9] among others has developed the approach in which a structure is replaced by a model consisting of a number of discrete masses and springs. The simplest such model is the single mass-spring system of Fig. 14(a). It is clearly important to know whether or not this simple model can give reasonable approximations to the deformations obtained from the complete analyses of beam problems such as those presented in this paper.

Considering only large plastic deformations, the spring is assumed to have the "rigid-plastic" load-deflection curve of Fig. 14(b). The displacement of the mass caused by a given dynamic load can then readily be worked out in terms of the yield force of the spring. The various quantities pertaining to the model are related to those of the prototype beam problem, the proper relationships being obtained easily by equating kinetic energies and works done by the respective force systems.

To obtain the correspondence one must assume a definite deflection curve for the beam; for large plastic deformations one would assume deflections to occur with a central plastic hinge. It is then evident that when the model quantities are replaced in the proper manner by the beam quantities, the results will be correct for the given beam problem when the beam actually deforms in the configuration assumed. The model analysis gives incorrect results when this configuration differs from the actual

one. Considering, for example, the problem of the simply-supported beam under uniform pressure, the errors in solving this problem by means of a one-dimensional model are precisely those of computing deformations from Eqs. (36) for all μ_o, instead of from Eqs. (37) in the range $\mu_o > 12$. The error in the mid-point deflection δ_f is not large, being less than 10 percent for μ_o less than 50. However, the central angle Θ_{of} predicted by the one-dimensional model is roughly double the value determined by the correct rigid-plastic analysis. This angle would appear to be important as a measure of the likelihood of rupture, but information from experiments is needed to clarify this point.

It should be noted that an analysis based on a single hinge configuration does not necessarily give an over-estimate of any deformation. In cases III and IV of this paper the single hinge analysis leads to values of central angle and deflection which are too low. These serve as counter examples against the general applicability of an assertion made in [4] to the effect that a plastic rigid analysis based on a single hinge model always yields an upper bound for the associated deformations.

The validity of the present results, as far as the neglect of elastic deformations is concerned, depends on how much the work done in plastic deformation exceeds the maximum possible wholly elastic strain energy that can be stored in the beam. This criterion can be put in the form

$$\frac{m\ell^3}{M_o^2\tau^2} E_p = f(\mu_o) > > \frac{T^2}{\tau^2}$$

where T is the fundamental period of vibration of the elastic beam. The function of μ_o on the left-hand side of the inequality is the dimensionless "plastic work" plotted in Fig. 13, the curves of which can be used according to the above inequality to estimate the probable range of μ_o or of τ required in order for the present results to hold. For non-rectangular force pulses the equivalent time T_o (defined by Eq. 38) should replace τ. Even when the above criterion is satisfied, the rigid-plastic analysis will not give the time history of the motion correctly, but this should not affect the usefulness of the predictions of final deformations. A brief discussion of some other sources of error is given in [8].

Bibliography

1. "Large Plastic Deformations of Beams under Transverse Impact" by E. H. Lee and P. S. Symonds. Journal of Applied Mechanics, Vol. 19, No. 3, 1952, pp. 308-315.

2. "Dynamic Load Characteristics in Plastic Bending of Beams", by P. S. Symonds. Journal of Applied Mechanics, Vol. 20, No. 4, 1953, pp. 475-482.

3. "A Note on Large Plastic Deformation of Beams under Transverse Impact" by T. H. H. Pian. M.I.T. Aero-Elastic and Structures Research Lab Report for ONR, Contract N5ori-07833, May, 1952. (Paper presented at Eighth-International Congress of Theoretical and Applied Mechanics, Aug. 20-28, 1952).

4. "Impulsive Motion of Elasto-Plastic Beams" by H. H. Bleich and M. G. Salvadori. Proceedings American Society of Civil Engineers, Separate No. 287, September, 1953.

5. "On the Development of Plastic Hinges in Rigid-Plastic Beams" by M. G. Salvadori and F. DiMaggio. Quarterly of Applied Mathematics, Vol. 11, No. 2, 1953, pp. 223-231.

6. "Plastic Deformations in Beams under Symmetric Dynamic Loads" by J. A. Seiler and P. S. Symonds. Tech. Report B11-13 of Brown University to ONR under Contract N7onr-35801, June 1953.

7. "Plastic-Rigid Analysis of Long Beams under Transverse Impact" by M. F. Conroy. Journal of Applied Mechanics, Vol. 19, No. 4, 1952, pp. 465-471.

8. "Impact of Finite Beams of Ductile Metal" by P. S. Symonds and C. F. A. Leth. Tech. Rept. B11-20 of Brown University to ONR, October 1953; to appear in Jour. Mechanics and Physics of Solids.

9. "Analysis and Design of Structures Subjected to Dynamic Loading" by N. M. Newmark Proceedings of Conference on Building in the Atomic Age, June 16, 17, 1952. Massachusetts Institute of Technology.

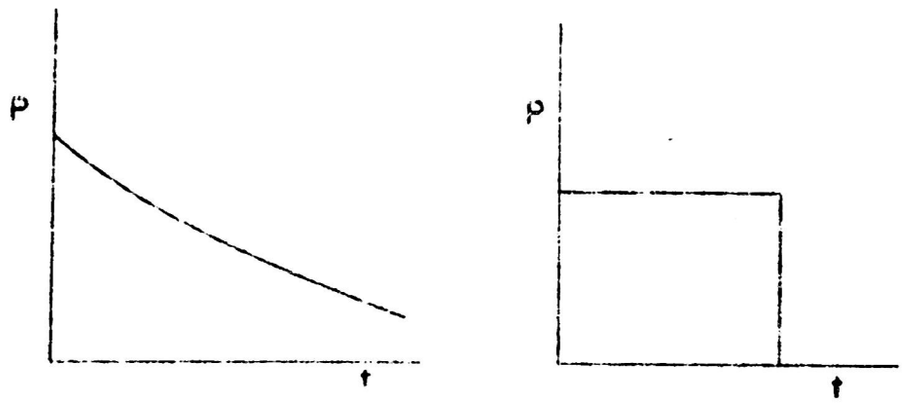

FIG. 1

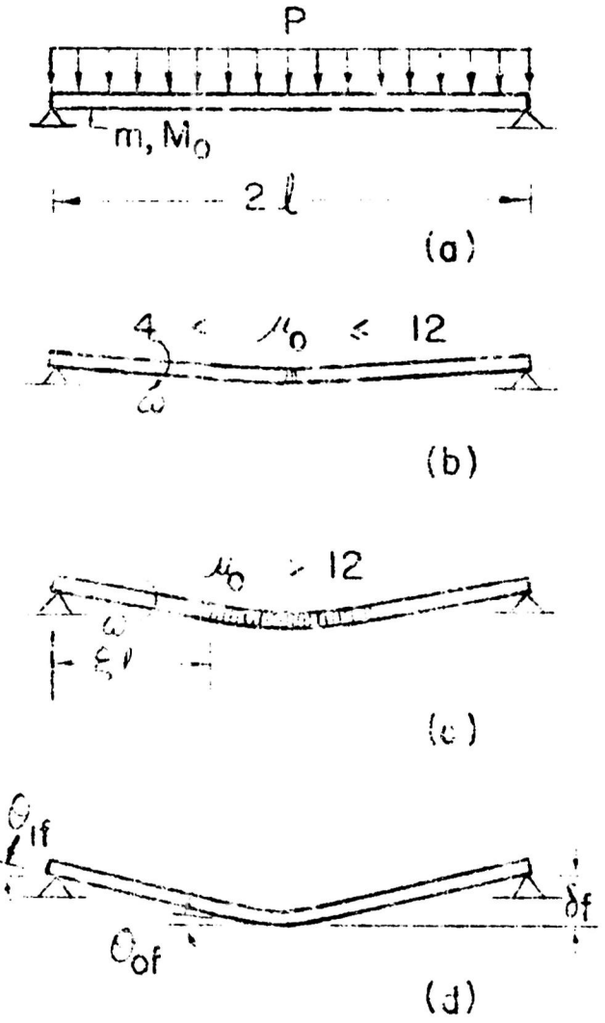

Case I

Fig. 2

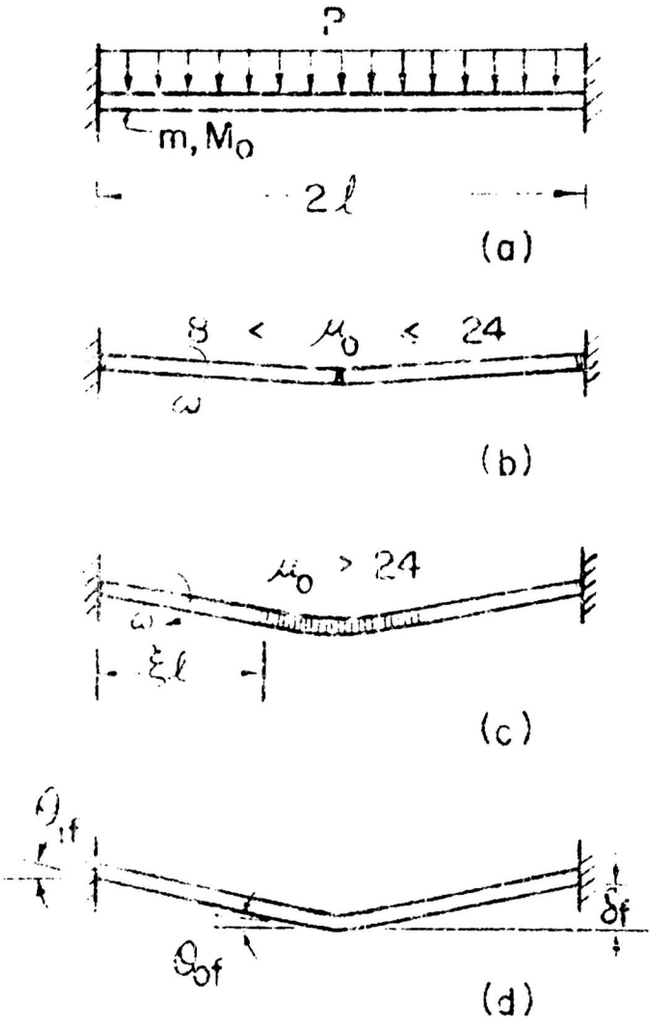

Case II

Fig. 3

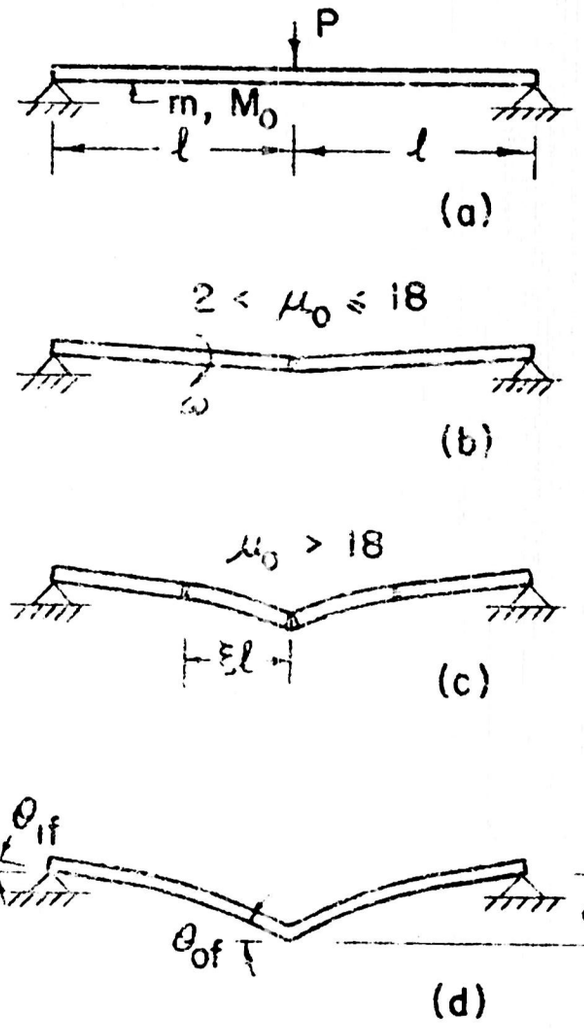

Case III

Fig. 4

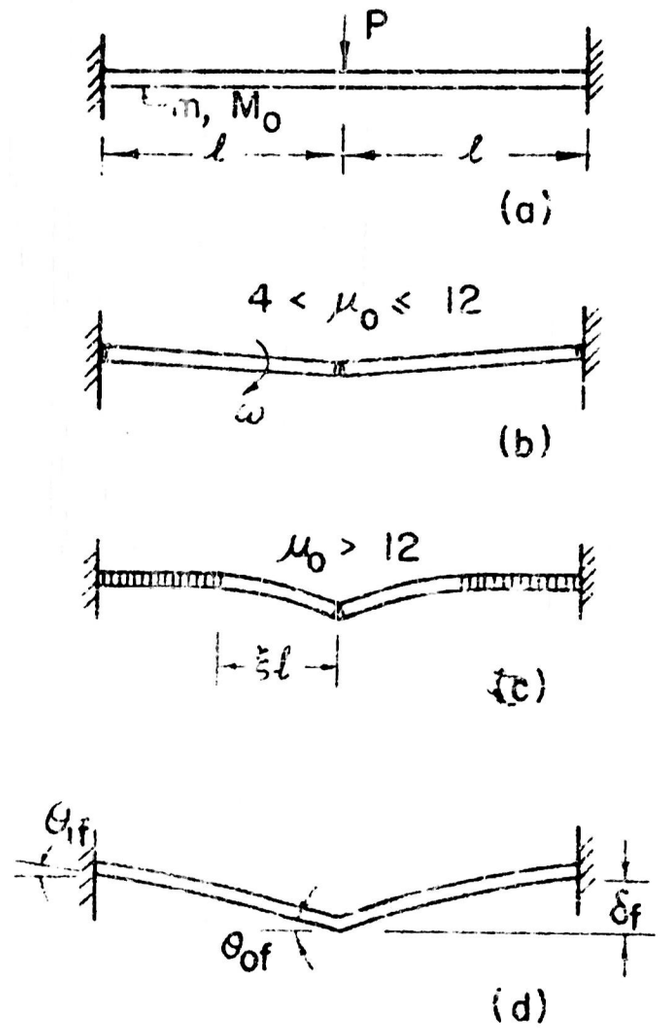

Case IV

Fig. 5

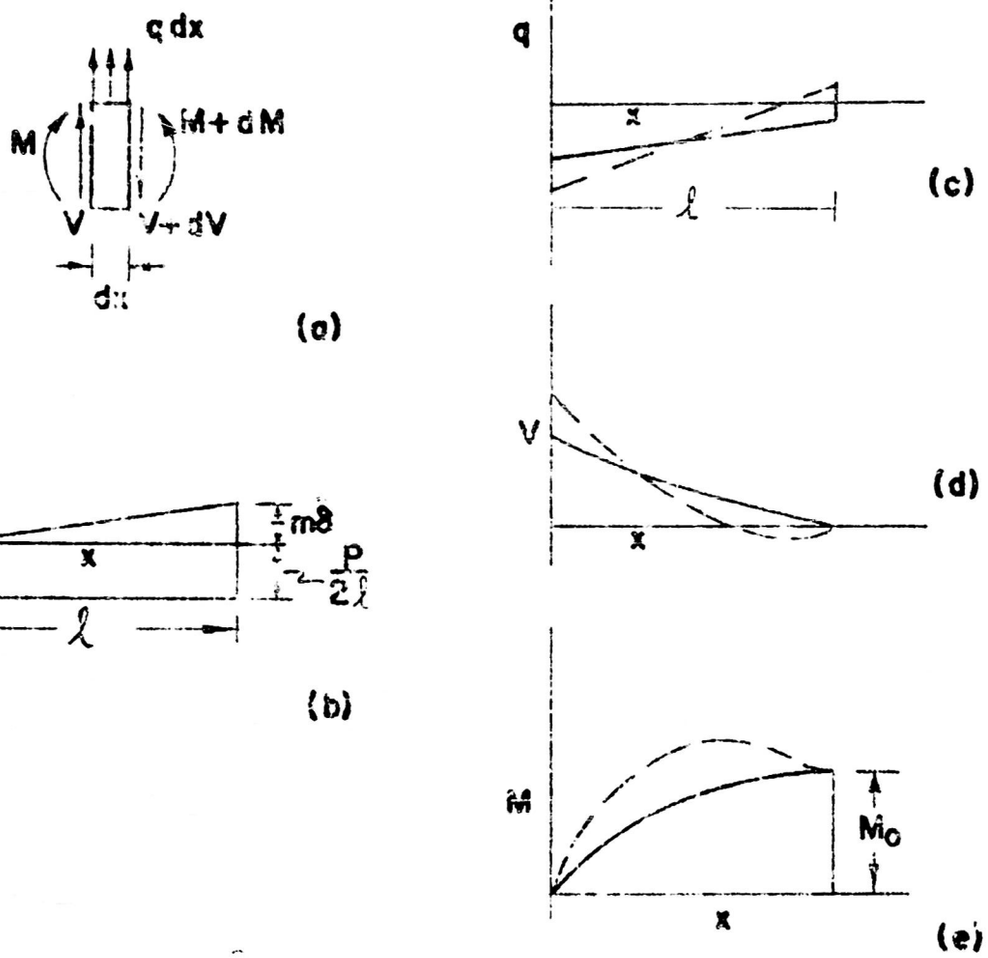

FIG. 6

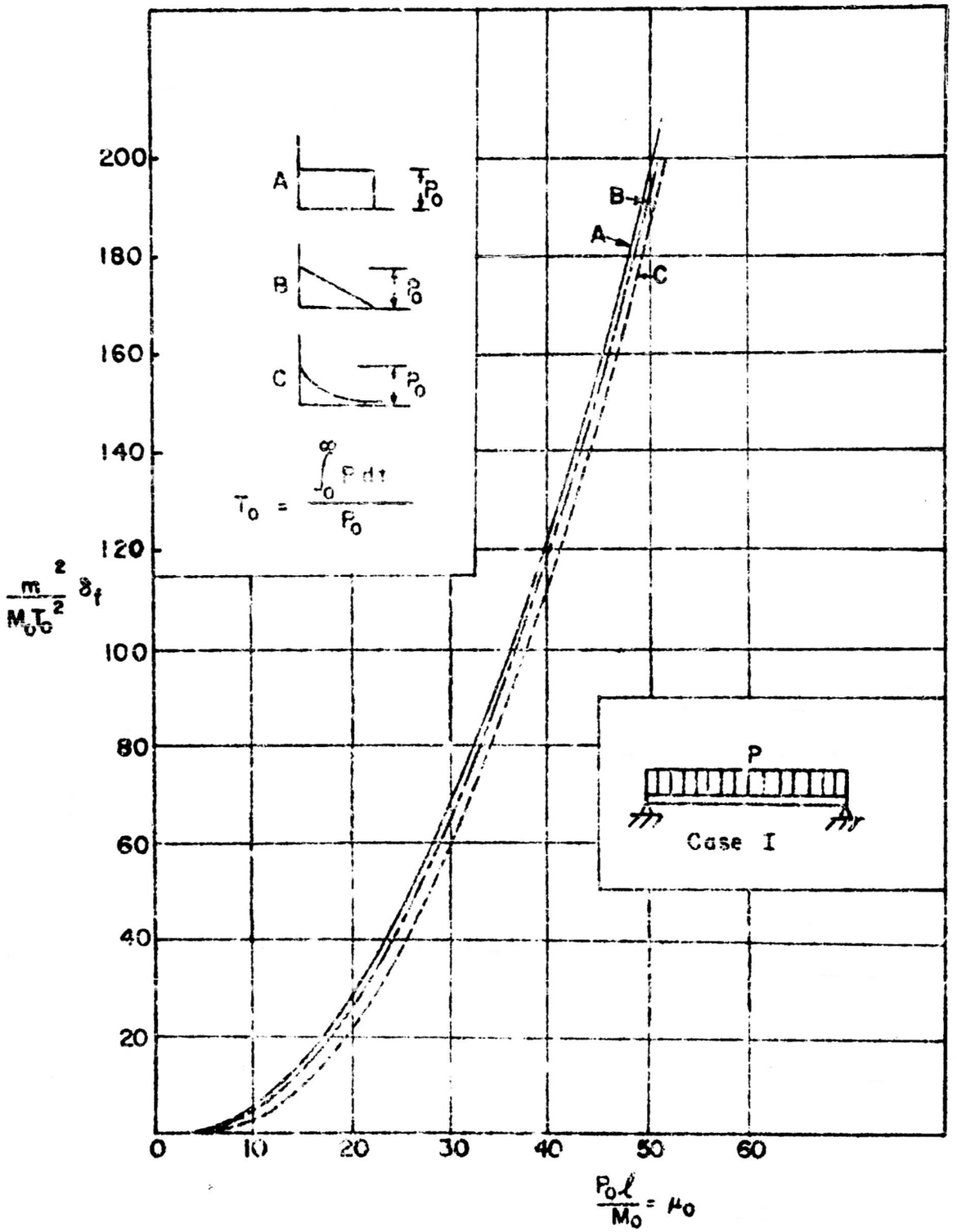
A
B
C
$T_0 = \frac{\int_0^\infty P\,dt}{P_0}$
200
180
160
140
120
100
80
60
40
20
0
10
20
30
40
50
60
$\frac{m^2}{M_0 T_0^2}\,\delta_f$
$\frac{P_0 \ell}{M_0} = \mu_0$
P
Case I

FIG. 7

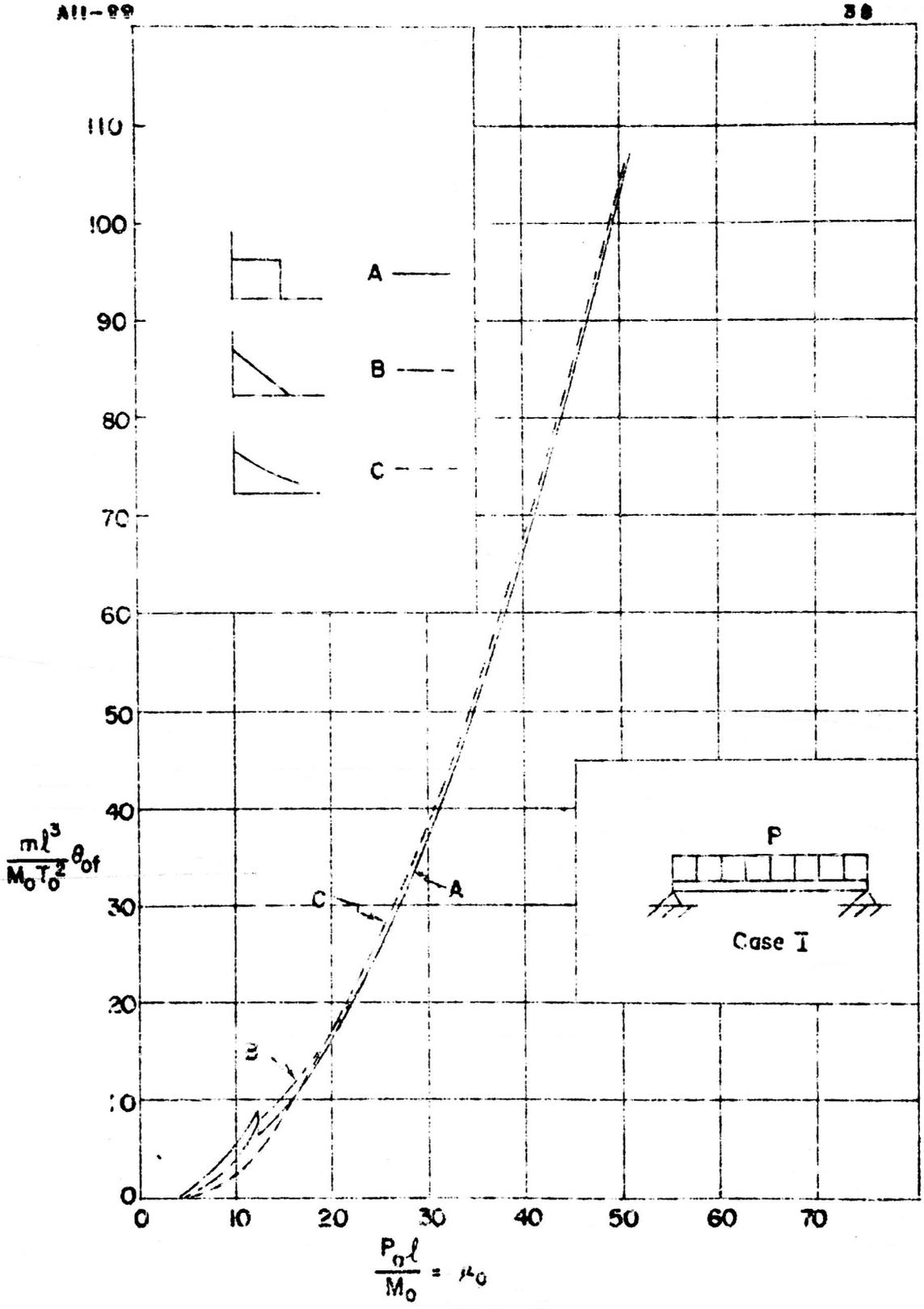
110
100
90
80
70
60
50
40
30
20
10
0
0
10
20
30
40
50
60
70
A
B
C
P
Case I
$\frac{m l^3}{M_0 T_0^2} \theta_{of}$
$\frac{P_0 l}{M_0} = \mu_0$

FIG. 8

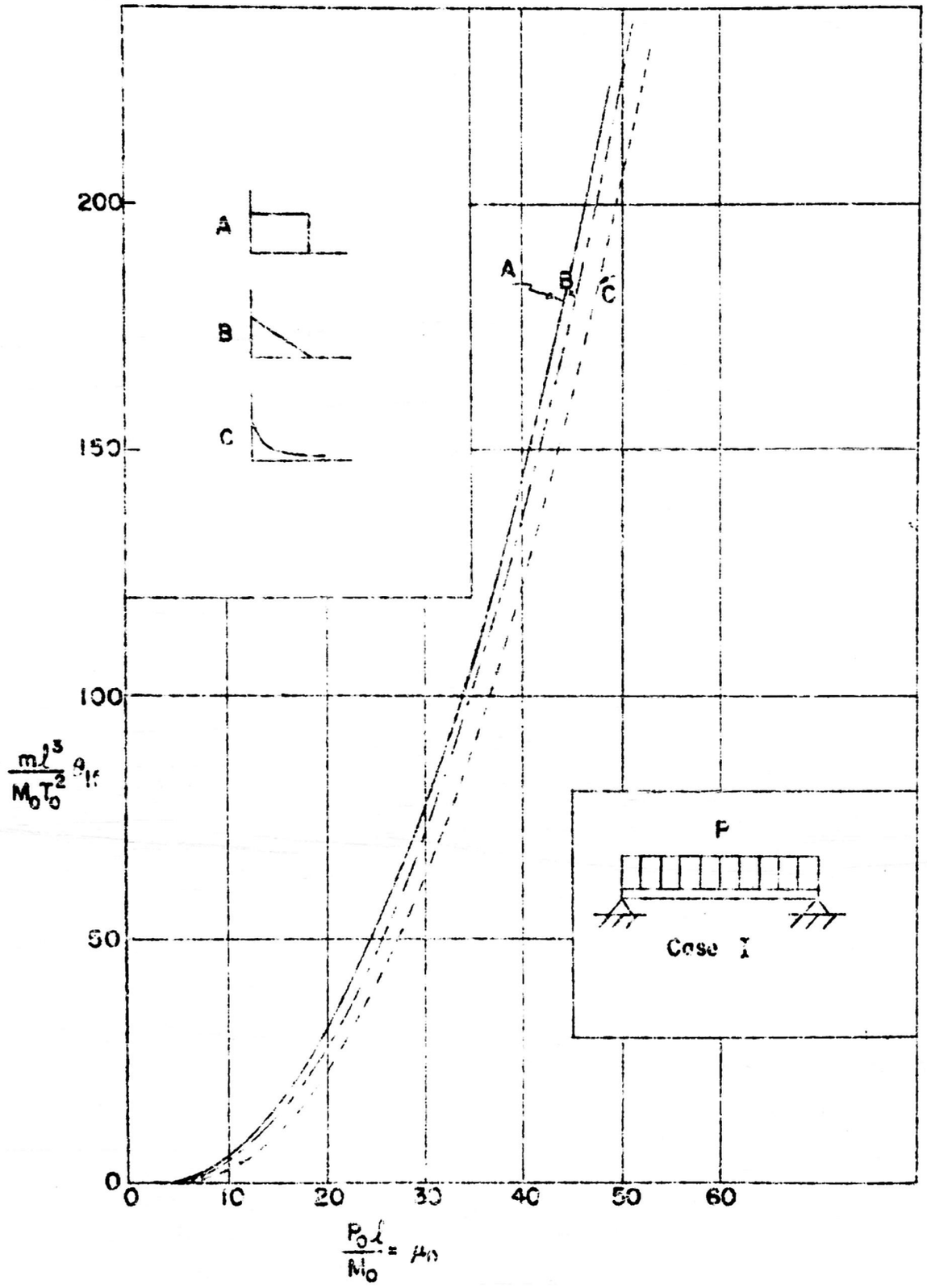
200
150
100
50
0
0
10
20
30
40
50
60
A
B
C
A
B
C
P
Case I
$\frac{m l^3}{M_0 T_0^2} \theta_{1c}$
$\frac{P_0 l}{M_0} = \mu_0$

FIG. 9

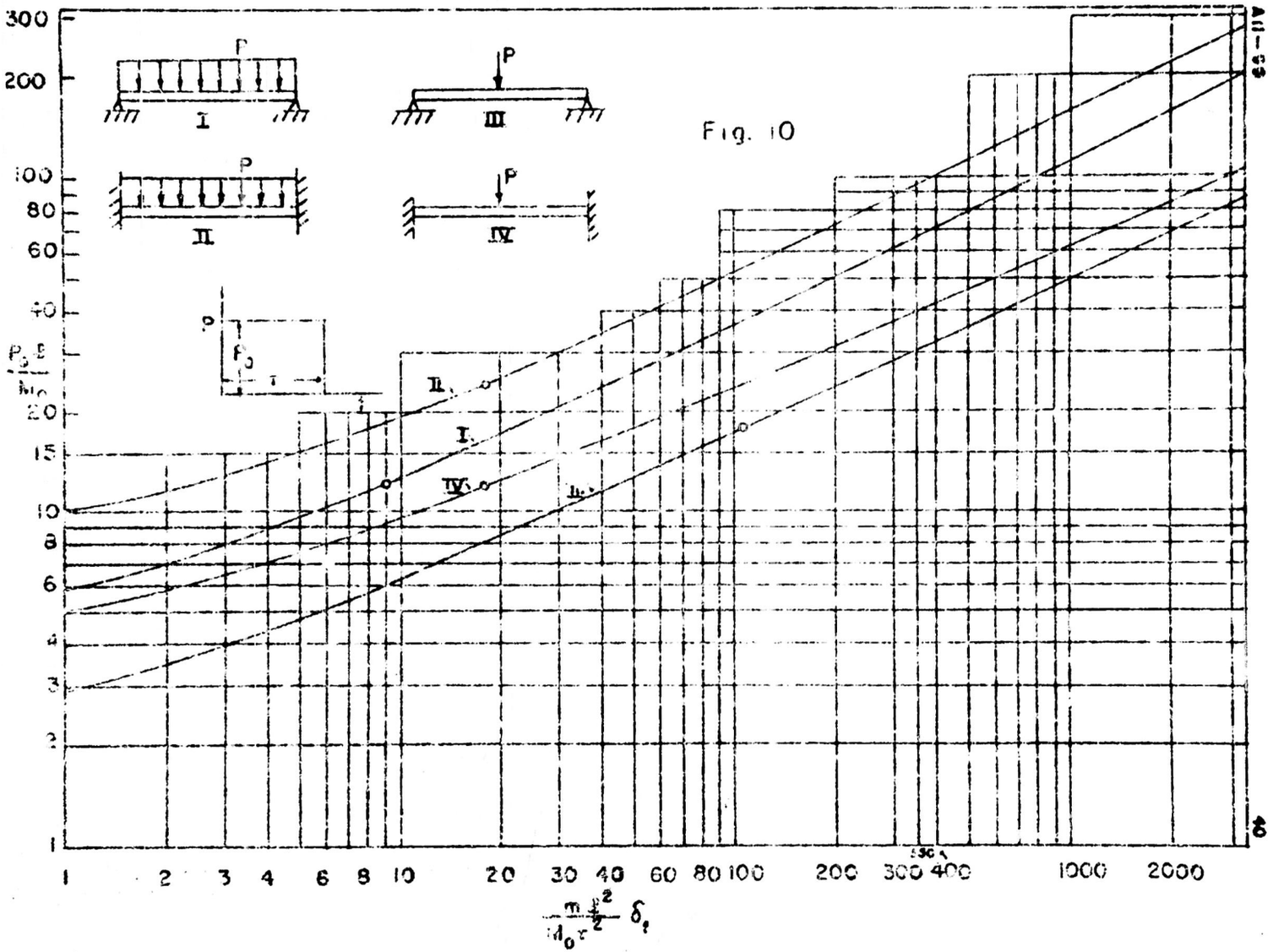
300
200
100
80
60
40
20
15
10
8
6
4
3
2
1
P
I
P
III
P
II
P
IV
p
P_0
τ
II
I
IV
III
1
2
3
4
6
8
10
20
30
40
60
80
100
200
300
400
1000
2000
$\frac{m}{M_0} \frac{l^2}{\tau^2} \delta_1$
$\frac{P_0 \delta}{M_0}$
δ

Fig. 10

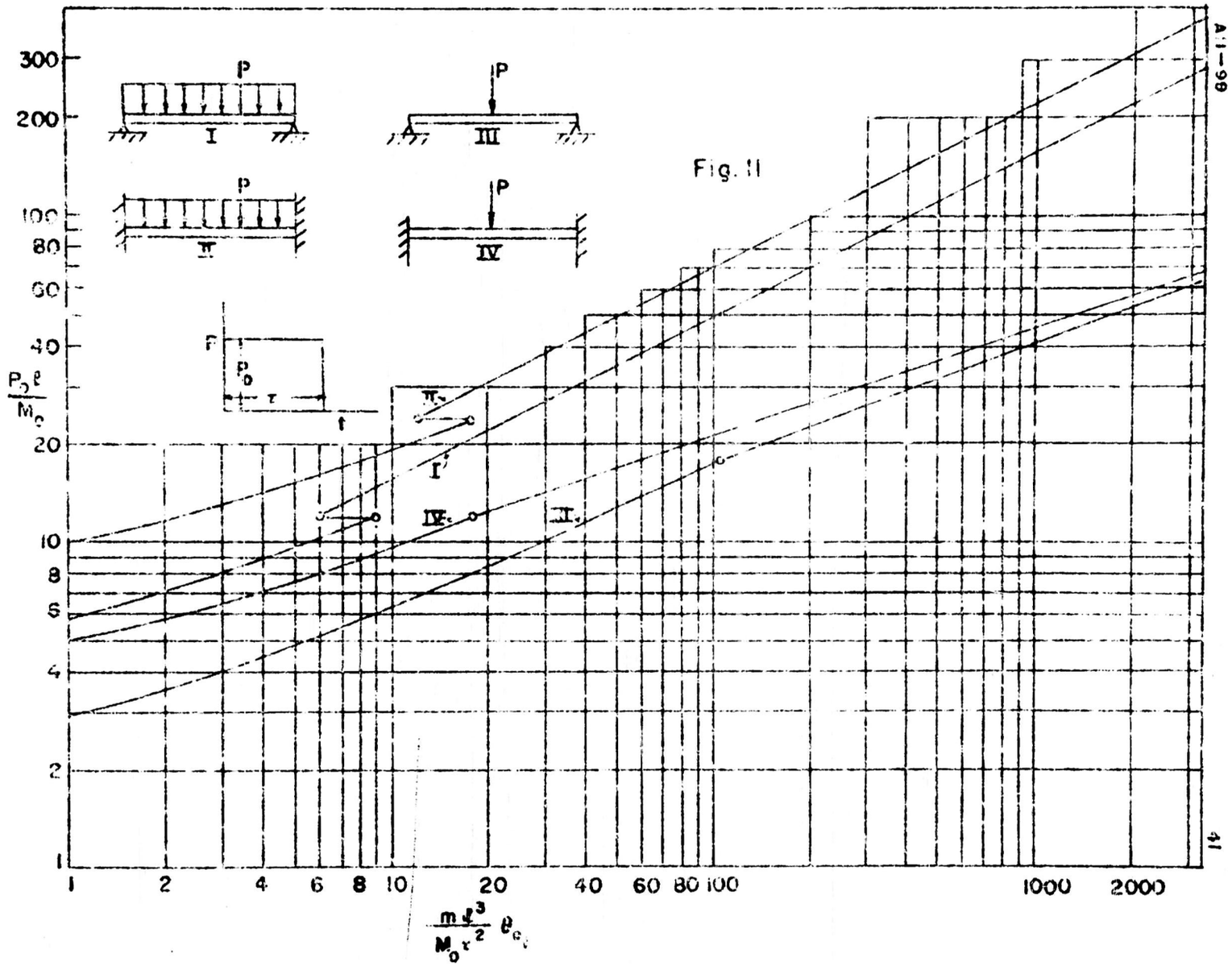
P
I
P
III
P
II
P
IV
F
P_0
τ
t
$\frac{P_0 \ell}{M_0}$
300
200
100
80
60
40
20
10
8
6
4
2
1
I'
II'
III'
IV'
1
2
4
6
8
10
20
40
60
80
100
1000
2000
$\frac{m \ell^3}{M_0 \tau^2} \theta_0$

Fig. 11

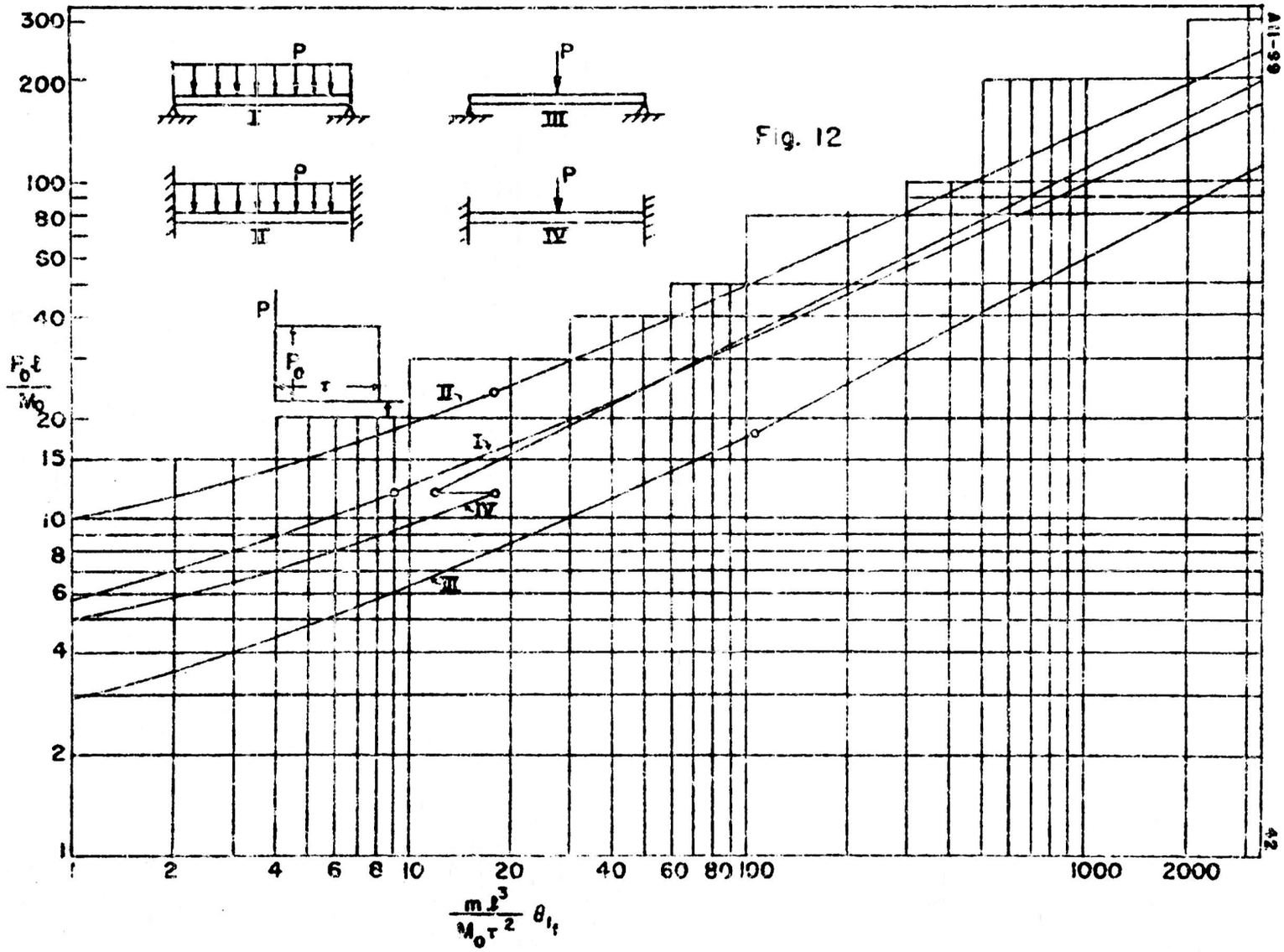
P
I
P
III
P
II
P
IV
P
P_0
τ
$\frac{P_0 \ell}{M_0}$
$\frac{m \ell^3}{M_0 \tau^2} \theta_{1_t}$
II
I
IV
III
300
200
100
80
60
40
20
15
10
8
6
4
2
1
2
4
6
8
10
20
40
60
80
100
1000
2000

Fig. 12

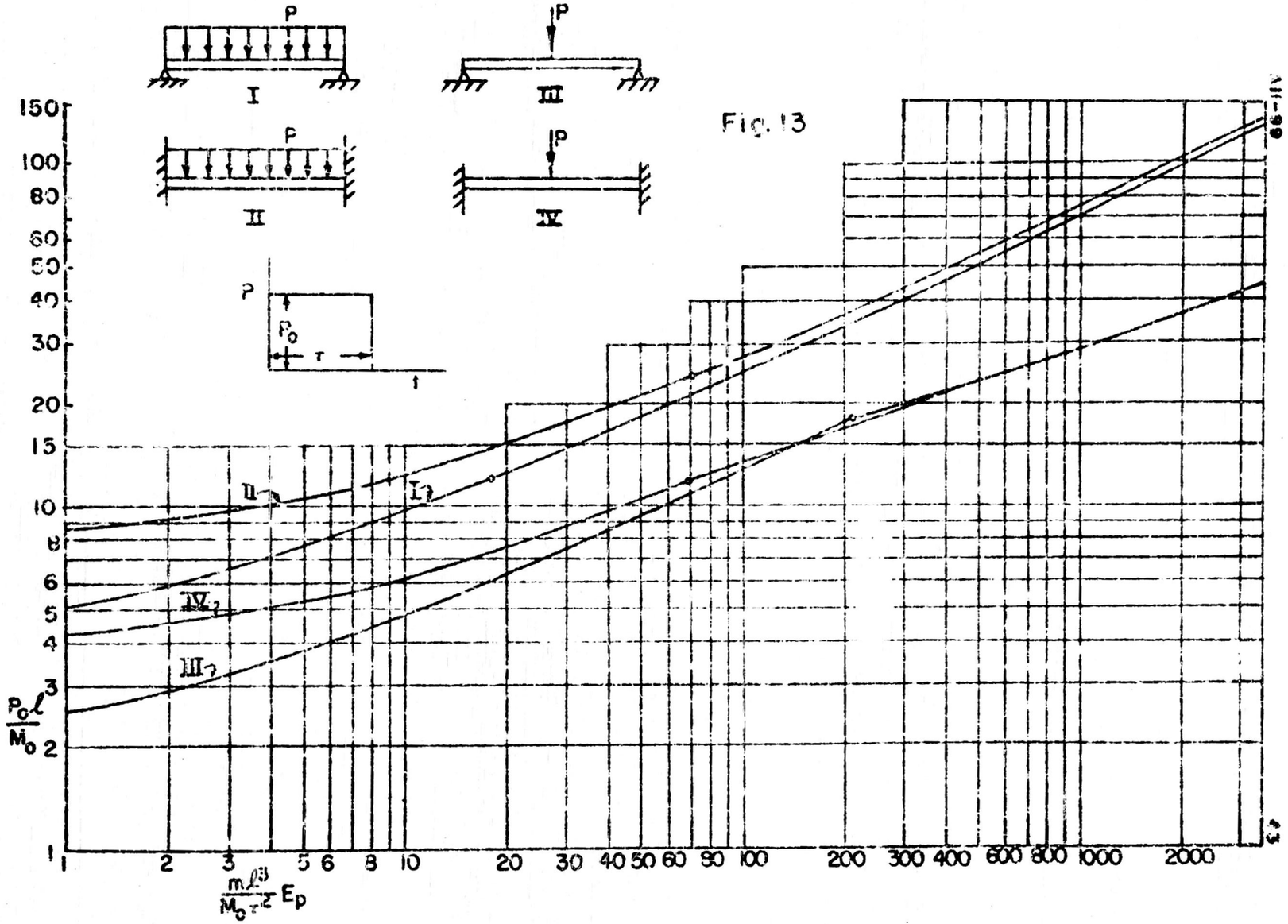
P
I
P
III
P
II
P
IV
P
P_0
τ
t
Fig. 13
II
I
IV
III
$\frac{P_0 l^3}{M_0}$
$\frac{m l^3}{M_0 \tau^2} E_p$
150
100
80
60
50
40
30
20
15
10
8
6
5
4
3
2
1
2
3
5
6
8
10
20
30
40
50
60
90
100
200
300
400
600
800
1000
2000

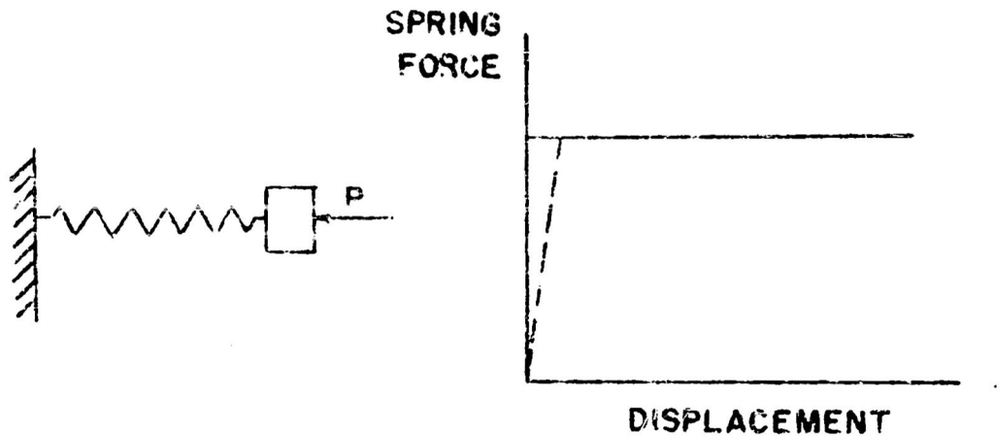

Fig. 14